

# Expanded Graphite–Epoxy Composites with High Dielectric Constant

Yun-Chuan Xie,<sup>1,2</sup> De-Mei Yu,<sup>1,2</sup> Chao Min,<sup>2</sup> Xiu-Sheng Guo,<sup>2</sup> Wei-Tao Wan,<sup>2</sup> Jing Zhang,<sup>2</sup> Hong-Lu Liang<sup>2</sup>

<sup>1</sup>State Key Laboratory of Electrical Insulation and Power Equipment, Xi'an Jiaotong University, Xi'an 710049, China

<sup>2</sup>Department of Applied Chemistry, School of Science, Xi'an Jiaotong University, Xi'an 710049, China

Received 24 January 2008; accepted 17 November 2008

DOI 10.1002/app.29741

Published online 11 March 2009 in Wiley InterScience (www.interscience.wiley.com).

**ABSTRACT:** Composites of an expanded graphite/diglycidyl ether of bisphenol A (DGEBA) were prepared by a simple melt blending method, and their dielectric and mechanical properties were investigated. During observations of fractured surfaces of the composites, the graphite sheets were seen to be homogeneously dispersed in the epoxy matrix. Moreover, the composites presented an enhanced dielectric constant ( $\sim 180$ ) and a low loss factor ( $\sim 0.05$ ) at 50 Hz, suggesting their potential suitability for embedded dielectric applications. The enhanced dielectric constant can be explained by the percolation theory and the rela-

tively low loss factor was attributed to strong interfacial interactions between the polymer molecules and the  $-\text{OH}/-\text{COOH}$  groups of the expanded graphite, which constrained the orientational polarization of the polarons. Furthermore, dynamic mechanical analysis of the composites showed a restricted macromolecular relaxation and improved mechanical properties. © 2009 Wiley Periodicals, Inc. *J Appl Polym Sci* 112: 3613–3619, 2009

**Key words:** expanded graphite; DGEBA; embedded dielectrics; percolation theory; high dielectric constant

## INTRODUCTION

Organic functional dielectrics with excellent dielectric properties are highly desirable for use in a wide range of applications, including high-energy density media and embedded dielectrics.<sup>1</sup> Dielectrics used for the newly developed embedded technique within the microelectronics industry require characteristics such as a small volume, good processability, a high dielectric constant ( $K$ ), and a low loss factor ( $\tan \delta$ ).<sup>2</sup> Single materials cannot satisfy all these requirements simultaneously, and previous research has to a large extent been focused on ceramic–polymer systems that adopt ferroelectric ceramics as high- $K$  fillers, e.g.,  $\text{BaTiO}_3$ , PZT, and PMN-PT.<sup>3–5</sup> The advantages of such composites include a predictable dielectric constant, a low loss factor, and an easy fabrication.<sup>6</sup> However, the  $K$ -value requirements (i.e.,  $K < 100$ ) for the composites could not be satisfied due to the low bulk dielectric constant of the polymer matrix ( $< 10$ ), as well as the high ceramic loadings ( $> 50$  vol %) deteriorating the mechanical properties of the

resulting composites. However, when using a percolation theory for the conductor–insulator composites, the observation of a dramatic increase in the  $K$  value close to the percolation threshold has attracted great interest. For instance, Zhang has reported an all-organic composite actuator materials with a high  $K$ -value of 400, when choosing copper-pthalocyanine as a high- $K$  filler<sup>7</sup>; Dang has found  $K$ -values of 400 in nickel–PVDF and CNTs–PVDF systems<sup>8,9</sup>; and Rao has obtained a  $K$ -value of 2000 in an epoxy resin filled with silver flakes.<sup>10</sup> Similar enhancements of the  $K$ -values in other metal–polymer systems have also been observed. Nevertheless, the benefits of these high- $K$  materials have unfortunately been counteracted by high dielectric loss factors, e.g., values of  $\tan \delta$  of 0.1, 0.4, and  $> 1$ .<sup>7,11–13</sup> Several researchers have reported on efforts to develop polymer composites with high  $K$  and low  $\tan \delta$  values. Xiong et al. used organic titanate as a coupling agent to engage a surface treatment of ceramic fillers, and the results indicated a suppressed dielectric loss as a result of a reduction of defects and an improved compatibility<sup>14</sup>; Wong et al. have reported on an epoxy resin filled with self-passivated Al particles, where the nano-scale insulating  $\text{Al}_2\text{O}_3$  layer gave rise to a high  $K$ -value of 109 and a low loss factor of 0.02 in the Al/epoxy composites.<sup>15</sup> Meanwhile, tiresome preparation processes and a poor flexibility of the composites have restricted their applications. Obviously, on the premise of an excellent processability, it is urgent to find a conductive filler/

Correspondence to: D.-M. Yu (dmyu@mail.xjtu.edu.cn).

Contract grant sponsor: Youthful Innovation Foundation of State Key Laboratory of Electrical Insulation and Power Equipment of China.

Contract grant sponsor: Postdoctoral Foundation of China; contract grant number: 2005038264.

polymer system with a low loss factor and a high dielectric constant to meet the practical requirements.

The present article reports on the use of expanded graphite (EG), inherent of a high aspect ratio and an excellent conductivity of the order of  $10^4$  S/cm, as a conductive filler when preparing EG/epoxy composites by a simple melt blending method. Dielectric measurements showed that the composites could be characterized with a high dielectric constant ( $\sim 180$ ) and a low loss tangent ( $\tan \delta < 0.05$ ) at 50 Hz, and such properties render them interesting to be used for embedded dielectrics. The dynamic mechanical properties of the composites were also investigated. Moreover, a mechanism for the electrical polarization and molecular relaxation processes, which are related to the interfacial interactions between the polymer network and the EG filler, was proposed.

## EXPERIMENTAL

### Sample preparation

The epoxy resin used in this study was a diglycidyl ether of bisphenol A, DGEBA (6101, Wuxi Chemical Materials Co. of Jiangsu province, China) with an equivalent weight of 250 g/equiv and an average molecular weight of  $M_n = 450$  g/mol. The curing agent was methyltetrahydrophthalic anhydride, MTHPA (Xi'an Resin Factory, Shaanxi province, China), and 2,4,6-tri(dimethylaminomethyl)phenol (DMP30, Shanghai Chemical Reagent Factory, Shanghai, China) was chosen as the accelerator. The intercalated graphite, that was oxidized and intercalated by nitric and sulfuric acid, was supplied from Qingdao Carbon Co. (China). Acetone, of chemical purity, was used as received from Xi'an Chemicals Factory (China).

The intercalated graphite was first dried in an oven at  $100^\circ\text{C}$  for 24 h to remove the moisture, and then placed in a muffle furnace at  $700^\circ\text{C}$  for 1 min to obtain the EG. The volume expansion ratio along the *c*-axis for the EG was about 200. A precalculated amount of EG was charged to a beaker and acetone was added. The resulting suspension was then sonicated for 30 min to form an EG–acetone slurry. The slurry was slowly added to the epoxy resin and stirred at  $80^\circ\text{C}$  for about 2 h, during which time most of the acetone was evaporated. Subsequently, the anhydride curing agent and DMP30 was added and the mixture was stirred vigorously for another 30 min. The mixture comprised of EG/epoxy/curing agent was degassed in a vacuum oven at  $40^\circ\text{C}$  for half an hour, then cured at  $100^\circ\text{C}$  for 2 h and post-cured at  $150^\circ\text{C}$  for 3 h. A series of EG/epoxy composites with EG loadings ranging from 0.5 to 5 wt % were fabricated. A blank epoxy sample was also pre-

pared for comparison. The densities used for calculating the volume content (vol %) of the fillers were: EG,  $2.26\text{ g/cm}^3$ ; epoxy,  $1.18\text{ g/cm}^3$ .

### Measurements

The fracture morphology of the EG/epoxy composites was studied using a JSM-2400 scanning electron microscope (Japan) with an accelerating voltage of 20 kV. The selected specimens were coated with a thin layer of gold prior to the SEM observations to avoid a charge buildup.

A Shimadzu wide-angle X-ray diffractometer (Japan), equipped with a graphite homochromatic instrument and a Cu anticathode (40 kV, 35 mA, scanning rate  $2^\circ/\text{min}$ ,  $2\theta = 10\text{--}70^\circ$ ), was employed to measure the diffracting patterns of the composites at ambient temperature ( $25^\circ\text{C}$ ).

Differential scanning calorimetry (DSC) was carried out on a Netzsh PC-200 DSC (Germany). The calorimeter had previously been calibrated with indium, and the heating rate was set to  $10^\circ\text{C}/\text{min}$ . All measurements were carried out under nitrogen atmosphere from room temperature to  $180^\circ\text{C}$ .

The thermal stability of the samples was evaluated by a Netzsh TGA-209C thermogravimetric analyzer (Germany) under  $\text{N}_2$  atmosphere with a heating rate of  $15^\circ\text{C}/\text{min}$  from room temperature to  $600^\circ\text{C}$ .

Samples,  $\sim 1\text{-mm}$  thick and 10 mm in diameter, were subjected to dielectric measurements with a parallel plate electrolyte method. The dielectric measurements were performed on a type-1296 dielectric interface connected to an SI-1255 HF frequency response analyzer from Solarton analytical (UK). All the measurements were performed in the frequency range of  $1\text{--}10^6$  Hz under room temperature. The dielectric strength of the samples was measured using a ball-rod electrode arrangement according to GB/T1408.1-99, with the alternative current of 50 kV and 50 Hz.

Dynamic mechanical measurements were performed on a DMA-Q800 analyzer (TA Instruments, USA). Samples were cut into  $35 \times 10 \times 1\text{ mm}^3$  sized rectangles. All experiments were performed in cantilever mode from 25 to  $180^\circ\text{C}$  at a heating rate of  $3^\circ\text{C}/\text{min}$ . The frequency for the experiments was 5 Hz.

## RESULTS AND DISCUSSION

### Fracture morphologies for the EG/epoxy composites

Figure 1 presents SEM micrographs of fracture surfaces of the composites with varying EG content. Figure 1(a) displays the morphology of the sonicated graphite sheets, evidencing that single sheets around

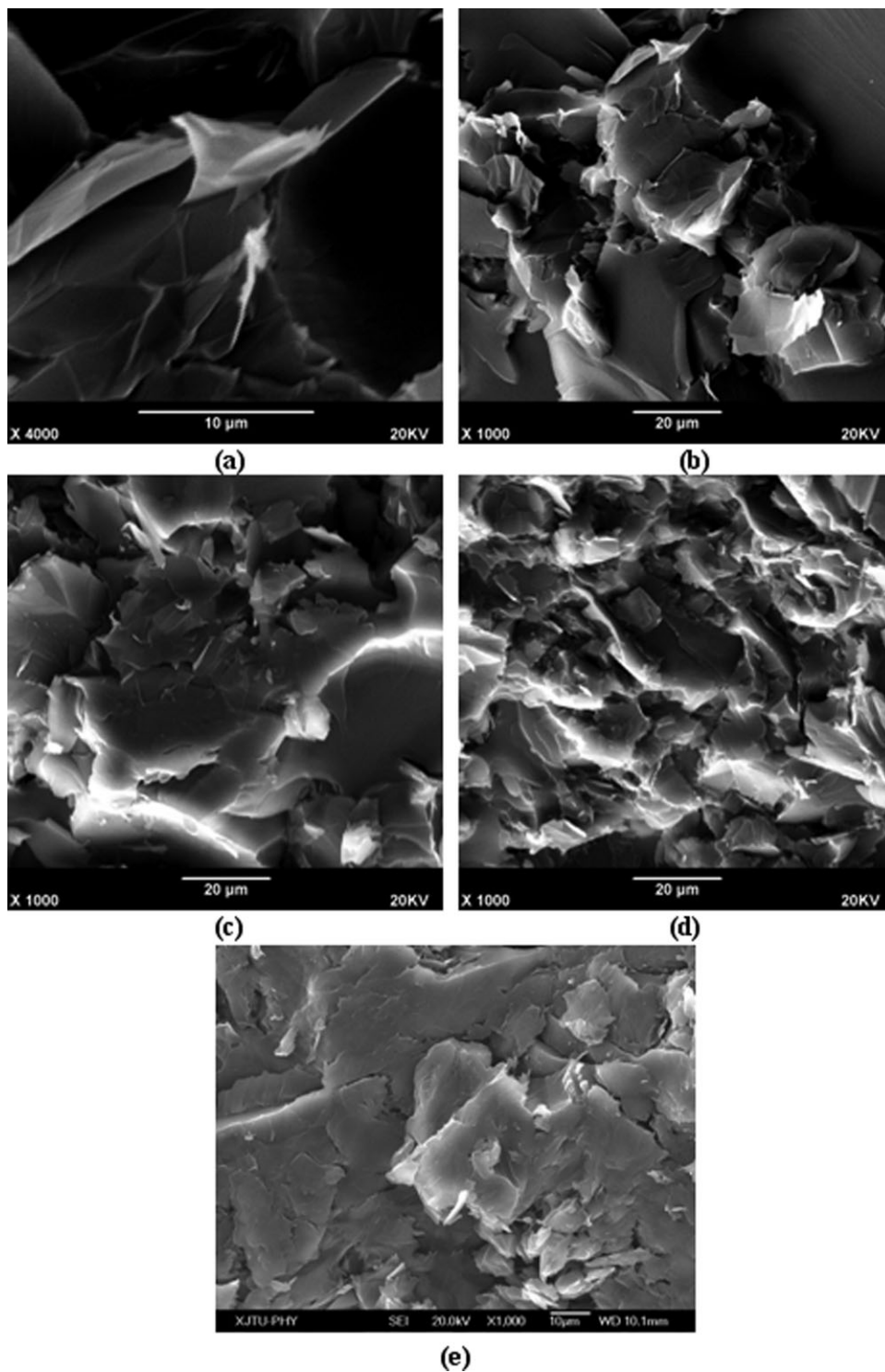


**Figure 1** SEM micrographs of (a) a single EG sheet, as well as of the EG/epoxy composites with varying EG fractions (b) 0.5 wt %, (c) 1.0 wt %, (d) 3.5 wt %, (e) 5 wt %.

20  $\mu\text{m}$  in width and 100 nm in thickness, could be obtained by the sonication treatment. Figure 1(b), (c) and (d), (e) show the morphologies of fracture surfaces for the composites with EG concentrations of 0.5, 1 and 3.5, 5 wt %, respectively. It was clear that except for sample with 5 wt % EG concentration, a majority of the graphite sheets could be well-dis-

persed in the epoxy matrix in the form of stacked layers.

#### WAXD patterns for the EG/epoxy composites

Figure 2 shows WAXD patterns for the EG/epoxy composites with varying EG fractions. The WAXD



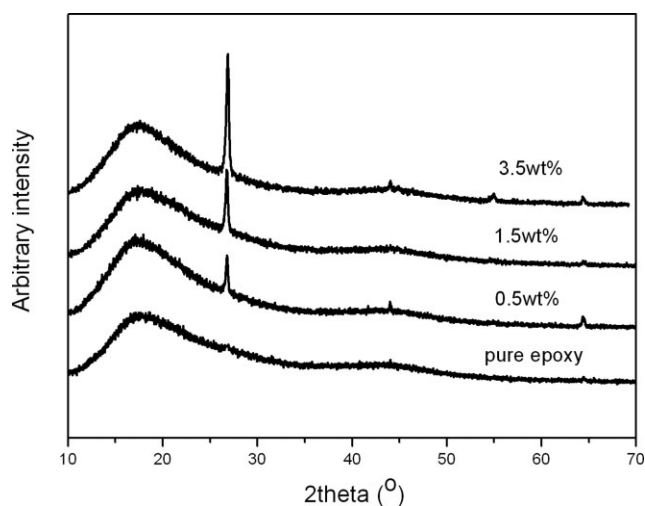


**Figure 2** WAXD patterns for the pure epoxy and EG/epoxy composites with varying EG fractions.

pattern for the neat epoxy was also given for comparison. Although neat epoxy displayed a broad diffraction peak at a  $2\theta$  of approximately  $16^\circ$ , the composites exhibited sharp peaks at  $2\theta$  of  $26.5^\circ$  (002), corresponding to the characteristic peak for neat graphite.<sup>16</sup> This result implied that a majority of the graphite sheets were still ordered or existed in multilayers, thus, maintaining their original  $d$ -spacing. It further suggested that the simple blending method used in this study was insufficient for exfoliating the graphite platelets into nanosheets as also reported elsewhere.<sup>17,18</sup> This conclusion was consistent with the morphology observations from Figure 1. With increasing EG concentration in the composites, the intensity of the peak at  $26.5^\circ$  became much stronger, which was attributed to a higher content of expanded graphite in the composites.

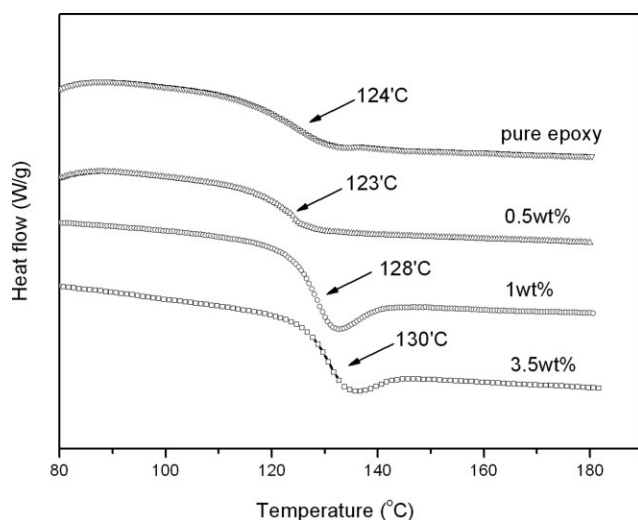


**Figure 3** DSC curves of the pure epoxy and EG/epoxy composites with varying EG fractions.

### Thermal behavior of the EG/epoxy composites

Figure 3 presents DSC heating curves of the composites as well as of the pure matrix. It can be seen that the glass transition temperature ( $T_g$ ) was  $124^\circ\text{C}$  for the pure epoxy matrix, and  $123$ ,  $128$ ,  $130^\circ\text{C}$  for the composites with  $0.5$ ,  $1$ ,  $3.5$  wt % EG fractions, respectively. When the EG concentration was low, a lubricant effect facilitated the movement of the molecular segments. However, with an increase in EG content, strong interfacial interactions between the two phases constrained the mobility of the molecules, which in turn led to increasingly elevated  $T_g$  values.

Table I lists the degradation temperature of the materials. The onset degradation temperature ( $T_{\text{onset}}$ ) and the maximum weight loss temperature ( $T_{\text{max}}$ ) of the composites were both found to be  $1$ – $5^\circ\text{C}$  higher than the corresponding values of the pure epoxy. This was assigned to the expanded graphite having a stacked structure composed of carbon atoms and thus an excellent heat resistance. As a result, the EG could block the heat transfer and improve the degradation temperature of the composites. Moreover, strong interfacial interactions between the two phases were also believed to be helpful in obtaining a higher degradation temperature.

### Dielectric properties of the EG/epoxy composites

Figure 4 displays plots of the dielectric constant ( $K$ ) versus frequency for the composite materials. It can be seen that the  $K$ -values of the composites varied from  $3.4$  to  $180$  as the EG concentration increased to  $3.5$  wt % at  $50$  Hz. At a  $5$  wt % EG loading, on the other hand, the  $K$ -value was significantly decreased to about  $70$ , and this drop was believed to be caused by air bubbles or cavities induced by the blending process during the preparation of the composite with high filler concentrations. Moreover, it was obvious that, for composites with higher EG loadings, the  $K$ -value was drastically lowered with increasing frequency. Two obvious steps were visible in the  $K$ -curves for the composites with EG concentrations of more than  $2.5$  wt %. As is well known, the main contributions to the  $K$ -values of the EG/epoxy composites are two polarizing processes.

**TABLE I**  
Degradation Temperatures of the Pure Epoxy and the Various EG/Epoxy Composites

Sample	$T_{\text{onset}}$ ( $^\circ\text{C}$ )	$T_{\text{max}}$ ( $^\circ\text{C}$ )
Pure epoxy	398	410
0.5 wt %	399	412
1.0 wt %	402	415
3.5 wt %	403	416

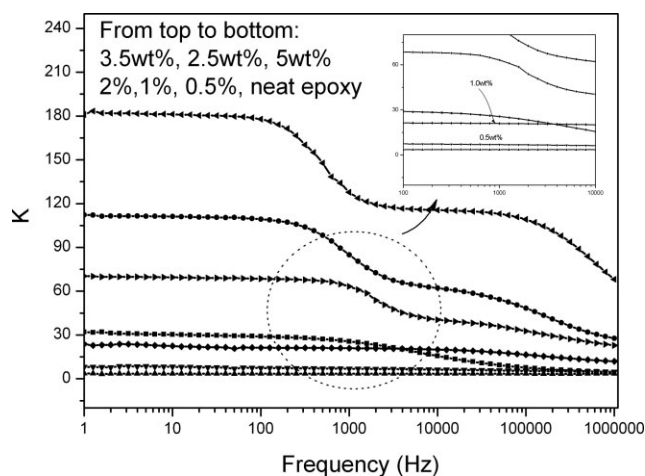


**Figure 4** The dielectric constants versus frequency for the various EG/epoxy composites.

The first is an interfacial polarization, which was induced through a local accumulation of free charges captured by defects or interfaces in the composites, and it relaxed at about  $5 \times 10^2$  Hz. The other is a molecular polarization, attributed to the polarization of electrons, atoms and various sized dipoles. Here, the polarization of the dipoles dominated the molecular polarization and it faded at about  $10^3$  kHz. The gradual decrease of these two polarizing processes was believed to cause the two step-wise reductions of the  $K$ -values with the increasing frequency, as can be clearly seen in Figure 4. As for the composites with lower EG concentrations (i.e., 0.5 and 1 wt %), no such steps were obvious from the figure.

Figure 5 shows the measured dielectric constant of the EG/epoxy composites as a function of the EG volume fraction. A moderate increase in  $K$ -values

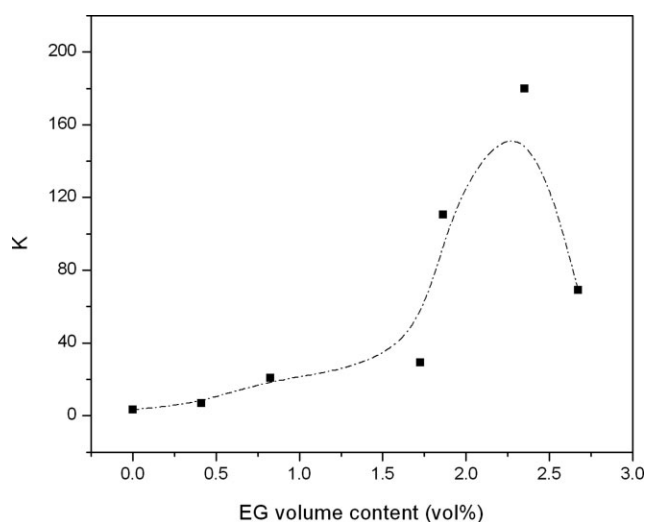


**Figure 5** The dielectric constants of the composites with varying volume fraction of EG.

was observed for EG loadings below 1.0 vol %, and a more significant increase occurred at concentrations above 1.0 vol %. At a frequency of 50 Hz and at room temperature, a maximum value of 180 was reached for the composite with  $\sim 2$  vol % (3.5 wt %) of EG. However, for EG loadings superior to 2 vol %, the  $K$ -value was drastically reduced, and this was believed to be caused by the increase in porosity of the composites. The abrupt increase in  $K$ -values at a volume fraction of 1.0 vol % EG, indicated the formation of a percolating network.<sup>13</sup> To estimate the percolation threshold concentration ( $v_c$ ), the experimental data were fitted with power laws for the composite near the percolation threshold<sup>8</sup>:

$$k \propto k_0(v - v_c)^x$$

Here,  $x$  is known to be the critical exponent for percolative transition of various dimensions. The best fits of the  $K$ -values were given by  $v_c = 0.98$  vol % and  $x = 2.17$ .

As expected, the percolation threshold for the EG/epoxy composites was much smaller than the  $v_c$  value of 16 vol % obtained for most conductor/insulator systems with micro-sized granular fillers, and the critical exponent,  $x = 2.17$ , differed from the typical value of  $\sim 2$  that can be calculated for three-dimensional composites with a classical statistical percolation model. For conductor/insulator composites, the  $v_c$  and  $x$  values are not only related to the bulk properties of the filler and matrix, but also to the filler shape and dispersion state.<sup>19</sup> The higher the aspect ratio of the filler, or the better the dispersion state of the filler, the smaller is the volume concentration needed to form a conductive pathway (see Fig. 6).

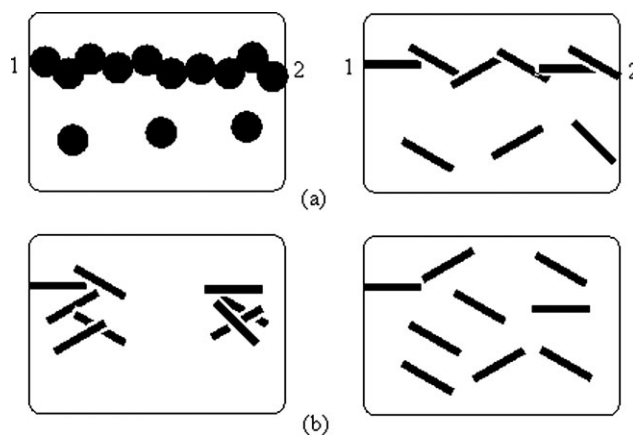


**Figure 6** A schematic plot of the effect of the filler shape on the conducting network in polymer composites; (a) a conductive channel: left-sphere shaped, right-sheet shaped, (b) dispersion states.

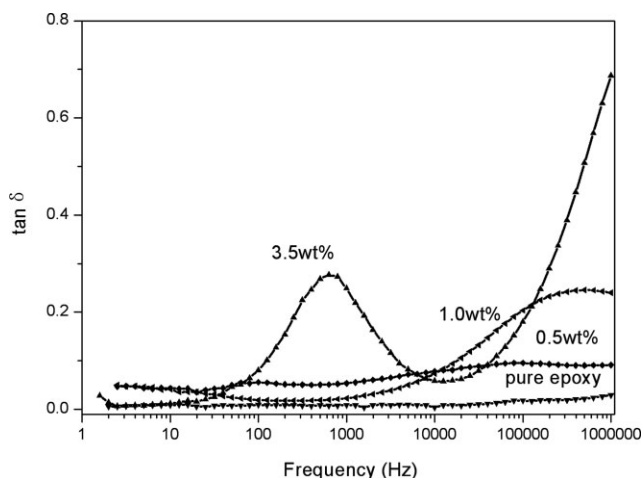


**Figure 7** The loss tangent for the pure epoxy and various EG/epoxy composites.

( $\sim 200$ ), it can readily form a conductive channel from point 1 to point 2 with a relatively low threshold. Other researchers have also observed this phenomena for similar EG/epoxy systems, and have found improved conductivities with an increase in EG content,<sup>20</sup> as well as low percolation thresholds for EG concentrations of  $\sim 3$  wt %.<sup>21</sup> A high aspect ratio and a good dispersion are key factors to obtain high- $K$  and low loss composites.

Figure 7 displays plots of loss tangent versus frequency for the studied materials. As can be seen, the loss factors for a majority of the composites were below 0.05 (at 50 Hz and room temperature). It is worth pointing out that as the EG fraction was increased to 5 wt %, the  $\tan \delta$  values became even lower (at 50 Hz). Generally, the total loss tangent is constituted of a conductive and a polarized part. Here, as the fraction of the conductive filler increased, the conductive loss also increased, and

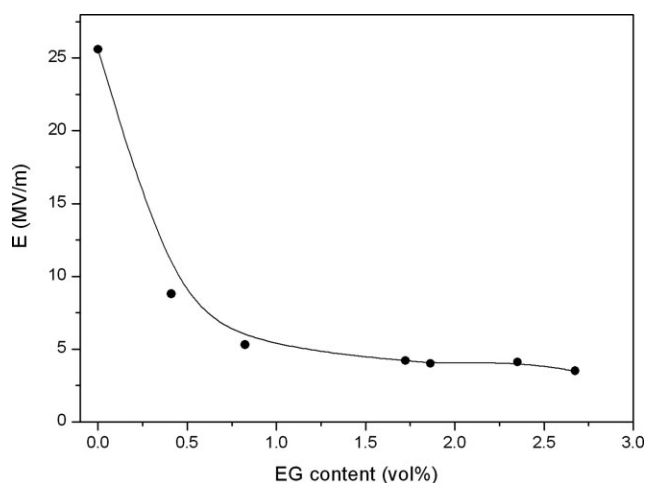


**Figure 8** The dielectric strength versus EG content for the EG/epoxy composites.

the low value of the total loss suggested a depressed polarized part. This can be explained by the existence of strong interfacial interactions, including hydrogen bonds and covalent linkages, between the epoxy molecules and the  $-\text{OH}/-\text{COOH}$  groups of the expanded graphite. These interactions constrained the turnarounds of the related polarons and lowered the total loss tangent.

Figure 8 demonstrates the dielectric strength of the various composites. As can be seen, the dielectric strength of the prepared EG/epoxy composites decreased with an increasing EG volume fraction. When the EG concentration was 0.4 vol %, the dielectric strength was lowered from 25.6 to 8.8 MV/m, due to the existence of conductive components. No abrupt shift in the breakdown voltage was observed, indicating an unchanged breakdown mechanism. In high electric fields, electrons of the composites can be accelerated, and an increasing number of electrons become excited through mutual collisions, thus inducing a so-called “electron avalanche” and thereby destroying the material.

#### Dynamic mechanical behavior of the EG/epoxy composites

Figure 9 presents the dynamic mechanical behavior of the neat epoxy material as well as its composites. The temperature position of the maximum of the loss modulus peak was taken as the glass transition temperature ( $T_g$ ) of the composite. At temperatures preceding the glass transition, it could be seen from the storage modulus-temperature curves that the dynamic modulus of the EG/epoxy composites was much higher than that of the neat matrix. The modulus decreased in the following order: 3.5 wt % > 1 wt % > 0.5 wt % > neat epoxy. And modulus of the composite with 3.5 wt % EG was as much as

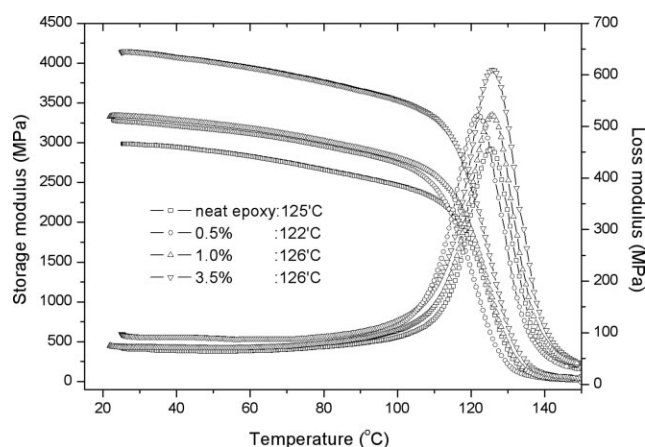


**Figure 9** DMA curves for the neat epoxy and the EG/epoxy composites.

40% higher than that of the pure epoxy matrix, and such an increased modulus was not only due to the fine dispersion of rigid EG sheets in the matrix, but also due to the crosslinking effect induced by the interfacial interactions between the polymer and EG. During the resin curing process, a hydrogen bond or covalent linkage between the epoxy molecules and the EG sheets was believed to have formed as a result of the existence of an —OH or —COOH functionality on the surface of the EG. Thereby, strong interactions between EG and the matrix were established. From the loss modulus-temperature curves, it is clear that, for an EG concentration of 0.5 wt %, the  $T_g$  was lowered by 3°C when compared with the neat epoxy, and this may have been caused by a lubrication effect of the EG sheets, thus facilitating the movements of the chain segments. However, with the increase in EG fraction ( $\sim 1$  wt %), the strong interaction between the epoxy molecules and the EG sheets may counteract this lubrication effect thus lowering the mobility of the chain moieties and causing an increase in  $T_g$ . This was in accordance with the loss tangent properties, as shown in Figure 7, in which the composite containing 0.5 wt % EG filler displayed relatively high  $\tan \delta$  value.

It can be seen from Figure 9, since the transition of the composite is related to the motions of chain segments, that the relative activity of the polymer molecules can be characterized by the intensity of the transition peak. Evidently, the intensity of the loss modulus for the composites was much higher than that of the neat epoxy, and it increased with an increasing EG fraction. This suggests that the mutual interaction between the polymer segments and the EG sheets became stronger with higher EG loadings. This was also consistent with the results from the dielectric measurements, suggesting that the dielectric and the dynamic mechanical properties of the composites were linked to each other through interfacial interactions.

In summary, the EG/epoxy composites reported herein were 2–3 type composites designed for embedded dielectrics applications. The enhanced dielectric constant ( $\sim 180$ ) and relatively low loss factor ( $<0.05$ ) rendered this material a promising candidate for use in embedded dielectrics. The interesting properties were attributed to a favorable combination of a high aspect ratio, a two-dimensional geometry, stiffness, and excellent conductivity of the EG material.

## CONCLUSIONS

In conclusion, percolative expanded graphite/epoxy composites could be prepared by a simple melt blending method, and showed promising potential for use in embedded dielectrics since they displayed not only enhanced dielectric and mechanical properties, but also a compatible processability and low cost. SEM observations showed that the graphite sheets were homogeneously dispersed in the epoxy matrix with a layered formation. The composites presented an enhanced dielectric constant of 180 as well as a low loss factor of 0.05 at 50 Hz. This improved dielectric constant can be explained by the percolation theory, and the relatively low loss factor can be attributed to strong interfacial interactions between the polymer molecules and the expanded graphite.

## References

1. Huang, C.; Zhang, Q. M. *Adv Mater* 2005, 17, 1153.
2. Bhattacharya, S. K.; Tummala, R. R. *J Mater Sci Mater Electron* 2000, 11, 253.
3. Xu, J. W.; Bhattacharya, S.; Pramanik, P.; Wong, C. P. *J Electron Mater* 2006, 35, 2009.
4. Dong, L. J.; Xiong, C. X.; Quan, H. Y.; Zhao, G. H. *Scrip Mater* 2006, 55, 835.
5. Rao, Y.; Wong, C. P. *J Appl Polym Sci* 2004, 92, 2228.
6. Cho, S. D.; Lee, S. Y.; Hyun, J. G.; Paik, K. W. *J Mater Sci Mater Electron* 2005, 16, 77.
7. Zhang, Q. M.; Li, H. F.; Poh, M.; Xia, F.; Cheng, Z. Y.; Xu, H. S.; Huang, C. *Nature (London)* 2002, 419, 284.
8. Dang, Z. M.; Lin, Y. H.; Nan, C. W. *Adv Mater* 2003, 15, 1625.
9. Wang, L.; Dang, Z. M. *Appl Phys Lett* 2005, 87, 042903.
10. Rao, Y.; Wong, C. P. *IEEE Proc Electro Comp Tech Conf* 2002, 920.
11. Wang, J. W.; Shen, Q. D.; Yang, C. Z. *Macromolecules* 2004, 37, 2294.
12. Huang, C.; Zhang, Q. M.; Li, J. Y.; Rabeony, M. *Appl Phys Lett* 2005, 87, 182901.
13. Li, Y. J.; Xu, M.; Feng, J. Q.; Dang, Z. M. *Appl Phys Lett* 2006, 89, 072902.
14. Xiong, C. X.; Chen, J.; Dong, L. J. *J Wuhan Univ Tech Mater Sci* 2001, 4, 82.
15. Xu, J. W.; Wong, C. P. *Appl Phys Lett* 2005, 87, 082907.
16. Yasmin, A.; Daniel, I. M. *Polymer* 2004, 45, 8211.
17. Chen, G. H.; Weng, W. G.; Wu, D. J.; Wu, D. C.; Chen, J. J.; Ye, L. H.; Yan, W. L. *Acta Polym Sinica* 2001, 6, 803.
18. Chen, G. H.; Wu, C. L.; Wu, D. J.; Weng, W. G.; Huang, S. X.; Lin, S. X. *Acta Polym Sinica* 2003, 5, 742.
19. Schueler, R.; Petermann, J.; Schulte, K.; Wentzel, H. P. *J Appl Polym Sci* 1997, 63, 1741.
20. Du, L.; Jana, S. C. *J Power Sources* 2007, 172, 734.
21. Jovic, N.; Dudic, D.; Montone, A.; Antisari, A. V.; Mitric, M.; Djokovic, V. *Scrip Mater* 2008, 58, 846.